Deep Learning on Flow Cytometry Data to Identify Clonal Populations for Myeloma Diagnosis

Thomas Ma
thomas.ma@emory.edu
Emory University
Decatur, Georgia, USA

Abstract

Deep learning to automate flow cytometry interpretations for disease diagnosis is an underexplored area, but it is an important direction for the medical field to offer pathologists a second opinion, catch myeloma early for better patient outcomes, and reduce the workload of all medical professionals involved in the data processing and interpretation of flow cytometry results. Convolutional neural networks (CNNs) and attention-based multiple instance learning (ABMIL) models have show promising results for flow cytometry interpretation. However, models have not been applied to myeloma detection, and CNNs and ABMIL models have not been evaluated against each other in a controlled experimental environment to determine the better architecture. We present an ABMIL approach that bags events from flow cytometry files, assigning bag-level labels, and an attention mechanism. The bagging of flow cytometry data allows the model to handle the high volume of events per file, and the attention mechanism allows the model to detect subtle differences in the flow cytometry data that would otherwise be lost due to the large context of an entire file. Our models are evaluated on our own new dataset, MM25, which contains data from patients at Emory University Hospital. Our ABMIL approach outperforms all other models tested, and it makes fewer false negative predictions compared to all other models tested, the key error of concern in medical diagnosis. To the best of our knowledge, we are the first work to compare the performance of CNNs and ABMIL models on flow cytometry interpretation and the first work to study the application of these models to myeloma.

Keywords

ABMIL, CNN, Myeloma, Flow Cytometry, Cancer Diagnosis

ACM Reference Format:
Thomas Ma. 2025. Deep Learning on Flow Cytometry Data to Identify Clonal Populations for Myeloma Diagnosis. In . CS 444: Deep Learning, Decatur, GA, USA, 7 pages. https://doi.org/10.1145/nnnnnnn.nnnnnnn

CS 444: Deep Learning, Decatur, GA, USA

ACM ISBN 978-x-xxxx-xxxx-x/YYYY/MM
https://doi.org/10.1145/nnnnnnn.nnnnnnn

1 Introduction

1.1 Background

1.1.1 Myeloma. Myeloma (or multiple myeloma) is a cancer of the plasma cells in the bone marrow. Healthy bone marrow will house normal plasma cells that make the expected antibodies, but malignant plasma cells produce an abnormal antibody called "M" protein. Although there is a slight risk of the disease running in family bloodlines, myeloma is generally not considered hereditary and instead develops from mutations that develop spontaneously with age.

The uncontrollable division of myeloma cells in the bone marrow results in abnormal complete blood count (CBC) results with decreased counts of red blood cells, white blood cells, and platelets. This can result in anemia (lack of oxygen), excessive bleeding, and a weakened immune system. The myeloma cells can also activate other cells in the bone marrow which can damage your bones, leading to bone pain or osteolytic lesions (weakened spots on the bones). This damage can increase risk of fractures and lead to hypercalcemia (increased levels of calcium in the blood). High levels of calcium and M protein in blood and urine can damage the kidneys and other organs, leading to impaired kidney function or kidney failure.

There is a 62.4% 5-year relative survival rate of myeloma patients diagnosed between 2015 and 2021, making it a difficult disease to beat with grim outlooks. It is currently incurable, but treatment through chemotherapy, immunotherapy, radiation therapy, etc. can put it into remission.

1.1.2 Flow Cytometry. Pathologists need a close examination to deliver a conclusive diagnosis to patients. For myeloma, flow cytometry is an important tool that provides valuable information about cells taken from a bone marrow biopsy. The cells from the sample are treated with antibodies that have fluorescent dyes attached. If a cell has a certain receptor, the antibody and fluorescent dye will bind to it. The cells are shot through a tube one by one, and a laser shows how light interacts with the cell. Based on this light, detectors will be able to gather details about the cell; forward scatter (FSC) measures cell size, and side scatter (SSC) measures internal structure and granularity. The fluorescent dyes will also light up, and detectors on the corresponding channels will receive information about the cluster of differentiation (CD) markers that can help determine the type of the cell (CD3 for T cells, CD19 for B cells, CD45 for leukocytes, etc.) and whether the cell is active (CD80, CD86).

Each flow cytometry instance is called a panel. When the data for a given panel is processed, each cell is called an "event". The

event contains numerical values for the cell information the panel tested for.

1.2 Motivation

Automation of flow cytometry interpretation is important because it can reduce the workload of pathologists and offer a "second opinion" when a pathologist is not completely certain of a diagnosis, yet it has been underexplored. Despite some developments in predictive models, automated flow cytometry interpretation is challenging because of the complexity of the data. Countless lab technicians are employed to process the data for visualization through "gating" cells of interest, and interpretation requires the specialized knowledge and experience of pathologists. Models struggle to detect abnormalities because of the often subtle differences in cell populations in the larger context of an entire panel, which can contain tens of thousands of events. Some studies have proposed convolutional neural networks and attention-based multiple instance learning models can apply to automated flow cytometry interpretation [7].

1.3 Approach

We present an attention-based multiple instance learning (ABMIL) [2] pipeline to handle the high volume nature of flow cytometry data. We hypothesize that the design of bagging all events in a file will resolve the issue of how large flow cytometry data is, and the application of attention will highlight areas of interest across flow cytometry samples that are positive for myeloma to allow detection of sutble population differences despite the large context.

1.4 Findings

Our ABMIL approach is evaluated on MM25, our own dataset, with traditional machine learning models (random forest) and other competitive deep learning models (convolutional neural network). Our experiments show that although we do not beat the external ABMIL baseline trained on leukemia data, our ABMIL approach outperforms all other models on our MM25 dataset.

1.5 Contributions

This work makes TWO main contributions as follows:

(1) We create a new dataset for studying deep learning-automated flow cytometry interpretation.
(2) We show AMBIL outperforms CNN in interpreting flow cytometry data.

To the best of our knowledge, this is the first work to compare CNN and ABMIL performance for deep learning on flow cytometry data in a controlled experiment. This work will lead to the development of automated flow cytometry interpretation systems.

2 Related Works

Although no work has explored the specific task of deep learning on flow cytometry data for the diagnosis of multiple myeloma, some previous studies have explored deep learning and flow cytometry data with other diseases.

2.1 Classical Machine Learning

Extensive work has been done that involves classical machine learning techniques for flow cytometry. One study [4] took a flow cytometry panel as input and applied a multivariate gaussian mixture model (GMM) to represent the individual events. A Fisher vectorization then transformed the output to a fixed-length phenotype representation. The authors used a support vector macine (SVM) to classify each patient into disease categories including acute promyelocytic leukemia (APL), acute myeloid leukemia (AML), acute lymphoblastic leukemia (ALL), and nonneoplastic cytopenia. The pipeline produced great results and even a subset of the parameters from a flow cytometry panel could achieve performance comparable to the full panel. This study shows that traditional machine learning can apply to flow cytometry data that has not been processed with gating or other data cleaning by lab technicians. However, because these models can only handle data that follows a strict structure, feature construction is required and results in the loss of information about rare subpopulations, subtle distributions, etc.

2.2 Convolutional Neural Networks

Convolutional neural networks (CNNs) fit better to flow cytometry data compared to traditional machine learning. One study [1] used a ResNet-50 on flow cytometry data and found high detection sensitivity for AML and B-ALL. However, the authors admit that the model had trouble identifying cells that are negative for the CD34 marker, leading to misclassifications for AML and B-ALL. The model made the same mistakes as would result from a manual human inspection. Despite this, the work demonstrates that CNNs show great potential for myeloma detection.

The authors also designed a new multi-level network architecture to classify cells for automatic gating, skipping the time-consuming and tedious process of manual gating done by lab technicians. This shows that deep learning models can be applied beyond disease detection and can generalize to other parts of the diagnostic process.

2.3 Attention-based Multiple Instance Learning

Attention-based multi-instance learning (ABMIL) models [2] have shown great performance on flow cytometry data [3]. In previous work, the data is extracted from flow cytometry files. 2-tube leukemia panels are provided as input to encoder neural networks that extract new features from the data in each respective tube. The new features analyzed by attention modules that designate a weight for each flow cytometry event based on the perceived importance of the event in the overall case diagnosis by the model. Weights, along with the new features, are used to extract pooled features from each tube. The pooled features from the 2 tubes are combined and analyzed by a final neural network, providing sample-level prediction for the case. The model produced exceptional results for detecting the presence of acute leukemia and even subtyping the disease. ABMIL models show great promise for deep learning on flow cytometry data because their structure handles data as bags, which is the native structure of flow cytometry files. The diagnosis of the patient provides the bag-level label, while the events of the file compose the bag. The nature of flow cytometry interpretation

as the detection of clonal populations cells lends itself well to the attention mechanism in the model.

3 Problem Formulation

Flow cytometry data contains a large set of cellular events, where each event corresponds to a single cell measured on d fluorescence or scatter channels. For a given patient or sample i, the raw file can be represented as

$$X_i = \{x_{i1}, x_{i2}, \ldots, x_{iN_i}\}, \qquad x_{ij} \in \mathbb{R}^d,$$

where N_i denotes the number of events in the sample. Note that files can contain a different number of total events. In flow cytometry files, it is common for

$$N_i \gg 10^5 \quad \text{or even} \quad N_i \approx 10^6.$$

The large amount of events per flow cytometry file creates several issues for models:

1. Computational and memory scaling. Most functions in machine learning and deep learning models have computational cost that scales at least linearly with N_i:

$$\text{cost}(f(X_i)) = O(N_i \cdot d).$$

For attention-based models, the cost is even higher due to pairwise interactions:

$$\text{cost}(f_{\text{attn}}(X_i)) = O(N_i^2).$$

2. Loss of population nuance. Flow cytometry data diagnosis often requires the location of smaller subpopulations that provide meaningful information about the pathology. Suppose a sample contains K cell subpopulations

$$\mathcal{P}_1, \ldots, \mathcal{P}_K,$$

each with probability mass p_k where $\sum_{k=1}^{K} p_k = 1$. If p_k is small (rare populations), then the number of observed events from population $\mathcal{P}_k$ is

$$n_k = p_k N_i.$$

For large N_i, n_k could be large, but since sampling is necessary to reduce the amount of events for each flow cytometry file so that the models can manage the volume of data, the effective representation of each population becomes

$$\tilde{n}_k = p_k M,$$

where $M \ll N_i$ is the number of events the models see. When p_k is small and M is limited by computational constraints,

$$\tilde{n}_k \approx 0,$$

causing rare or subtle populations to become invisible to the model because of the large context. However, even without sampling or minimal sampling, models that do not compensate for the potential that a few small subpopulations could determine the presence of a disease will have a hard time detecting abnormalities because of large N_i in flow cytometry files.

4 Approach

4.1 Preprocessing and Models

As discussed in section 3, flow cytometry files can contain tens of thousands of events. This requires additional design elements to ensure that the models can handle the large volume of data.

4.1.1 Traditional Machine Learning. Traditional machine learning models cannot handle raw flow cytometry data since we want to detect myeloma for a patient, but there are tens of thousands of events in each file. Instead, we implement feature engineering to transform events into representative values. We choose random forest combined with summary statistics (Algorithm 1) and clustering approaches (Algorithm 2) as suitable feature engineering pipelines due to success in previous work [5] [6].

Algorithm 1 Flow Cytometry Events to Summary Statistics

function SUMMARIZE(E)
  Input: Events $E = \{e_1, \ldots, e_N\}$, $e_i \in \mathbb{R}^d$
  Output: Summary feature vector S
  for $j = 1 \to d$ **do**
    for $i = 1 \to N$ **do**
      $x_{ij} \leftarrow T_j(e_{ij})$ ▷ Apply marker-wise transform
    end for
    $\mu_j \leftarrow \frac{1}{N} \sum_{i=1}^{N} x_{ij}$
    $\text{median}_j \leftarrow \text{median}\{x_{1j}, \ldots, x_{Nj}\}$
    $\sigma_j^2 \leftarrow \frac{1}{N} \sum_{i=1}^{N} (x_{ij} - \mu_j)^2$
    for each quantile level $p \in P$ **do**
      $q_{j,p} \leftarrow \text{quantile}(\{x_{1j}, \ldots, x_{Nj}\}, p)$
    end for
  end for
  $N_{\text{total}} \leftarrow N$
  $S \leftarrow \text{concat}(\mu_j, \text{median}_j, \sigma_j, q_{j,p}, N_{\text{total}})$
  return S
end function

However, these approaches do not capture the nuances in the flow cytometry data. The summary statistics cannot represent any subpopulations and will only convey general information about the cells to the model. Clustering can capture populations and even detect subtle populations, but it is difficult to tune the hyperparameters so that the model is not overly sensitive to normal populations but sensitive enough so that it can detect abnormal populations.

4.1.2 Convolutional Neural Networks. Convolutional neural networks can work directly with the native structure of the flow cytometry data, seeing the events. However, sampling is needed to ensure that the model could handle a set size of the data, and the data must be converted to image shape so that the model can handle the dimension of the data.

4.1.3 Attention-based Multiple Instance Learning. Attention-based multiple instance learning models can also work with the native events of flow cytometry data, but they can handle a larger amount of events per flow cytometry file through bags as in Algorithm 3. Bags are assigned a label which applies to all events inside so that the model is not analyzing every single event.

Algorithm 2 Flow Cytometry Events to Clusters

function CLUSTER(E, K)
  Input: Events $E = \{e_1, \ldots, e_N\}$, number of clusters K
  Output: Cluster feature vector F
  for $j = 1 \to d$ **do**
    for $i = 1 \to N$ **do**
      $x_{ij} \leftarrow T_j(e_{ij})$
    end for
  end for
  $X \leftarrow [x_{ij}] \in \mathbb{R}^{N \times d}$
  labels $\leftarrow C(X, K)$ ▷ Apply clustering algorithm
  for $k = 1 \to K$ **do**
    $I_k \leftarrow \{\, i \mid \text{labels}_i = k \,\}$
    $n_k \leftarrow |I_k|$
    $p_k \leftarrow n_k / N$
    for $j = 1 \to d$ **do**
      $\mu_{kj} \leftarrow \frac{1}{n_k} \sum_{i \in I_k} x_{ij}$
      $\text{median}_{kj} \leftarrow \text{median}\{x_{ij} : i \in I_k\}$
    end for
    $f_k \leftarrow \text{concat}(p_k, \mu_{kj}, \text{median}_{kj} \text{ for all } j)$
  end for
  $F \leftarrow \text{concat}(f_1, f_2, \ldots, f_K)$
  return F
end function

Algorithm 3 Flow Cytometry Events to Bags

function BAG(E, B, m)
  Input:
- Events $E = \{e_1, \ldots, e_N\}$
- number of bags to generate B
- number of events per bag m

  Output: Set of bags $\mathcal{B} = \{\, \mathcal{B}_1, \ldots, \mathcal{B}_B \,\}$
  Initialize $\mathcal{B} \leftarrow \emptyset$
  for $b = 1 \to B$ **do**
    Sample an index set

$$I_b \subset \{1, \ldots, N\}, \quad |I_b| = m$$

    Construct bag

$$\mathcal{B}_b \leftarrow \{e_i : i \in I_b\}$$

    Add bag to collection:

$$\mathcal{B} \leftarrow \mathcal{B} \cup \{\mathcal{B}_b\}$$

  end for
  return $\mathcal{B}$
end function

4.2 Dataset

We introduce a new dataset, MM25, composed of flow cytometry files in flow cytometry standard (.fcs) format sourced from the Department of Pathology and Lab Medicine at Emory University Hospital over three years (2019-2022). The flow cytometry files are paired with data from the hospital electronic health record (EHR) which includes textual interpretations from pathologists that reviewed each case.

Label	Samples
No clone detected (0)	5147
Clone detected (1)	2226
Ambiguous (2)	58

Table 1: Breakdown of MM25 dataset composition.

4.2.1 Preprocessing. Flow cytometry files for cases not related to myeloma were discarded, resulting in a total of 7431 files remaining. The file names contained patient names and specimen numbers, so they were de-identified and a mapping was created so that individual cases could still be traced back to a patient for analysis.

The textual interpretations were parsed for keywords to produce labels. Interpretations with keywords such as "fails", "failed", "fail", and "no definite" indicated no clonal population present, the negative class. Interpretations with keywords such as "unique", “clonal”, “demonstrates the presence”, “reveals”, “distinct population”, “neoplastic plasma”, “plasma cell neoplasm”, “myeloid”, “no aberrant” indicated the presence of a clonal population, the positive class. Cases that did not fall into either were classified as ambiguous and discarded. The class sizes are shown in Table 1.

4.2.2 Quality. The use of keywords to label the data presents the potential that misclassified data is fed to the models. Some manual inspection was completed, and a few examples of misclassified data were found and re-assigned the appropriate labels. However, the dataset as a whole still likely contains some misclassified cases. Improvements to the labeling process could be made to provide more confident labels for each flow cytometry file.

4.2.3 Sourcing. The data was sourced from the Department of Pathology and Lab Medicine with the help of Dr. David Jaye and Dr. Brooj Abro. We received formal approval through the IRB, and the management of the data is HIPAA compliant.

As an informal note at the request of Dr. Yang, I will share the details of how I obtained the data. I had the opportunity to work with real hospital medical data as an undergraduate after becoming acquainted with these two pathologists through shadowing in preparation for medical school. It is important to simply speak about or even briefly mention your areas of experience or expertise, since they revealed to me they were very interested in the development of AI. The medical domain still has tons of room for improvement and a surprising lack of research, so many doctors will be open to new ideas and research, even if it isn’t part of their job.

5 Experiments

5.1 Data

All models were evaluated on our own MM25 dataset as described in section 4.2. A subset of 2040 flow cytometry files was used to reduce model training and inference time. We choose a 60/20/20 split to remain consistent with previous work [3] and the standard for most medical machine learning and deep learning models.

We sample 2048 events per file for CNN to reduce computation time. We sample bags of 15000 events per file for ABMIL based on previous work [3]. For both models, we do sampling without

Table 2: Data Split for Experimental Subset

Set	Samples
Training	1215
Development	405
Test	405

replacement unless the bag is below the 15000 event threshold, where we sample with replacement.

5.2 Models

The following four models are experimented:

- Random forest with summary statistic features (Section 4.1.1)
- Random forest with clustering features (Section 4.1.1)
- Convolutional neural network (Section 4.1.2)
- Attention-based multiple instance learning (Section 4.1.3)

The models are evaluated with precision, recall, F1-score, AUROC, and accuracy.

The random forest models are set to 200 estimators. The CNN is trained for 10 epochs using a learning rate of 1×10^{-3}, Adam optimizer, and batch size of 8. The ABMIL model is trained for 20 epochs using a learning rate of 1×10^{-4}, Adam optimizer, and a batch size of 4.

All models were trained across all epochs without early stopping, but only the best model was saved for each.

Our experiments are run on a single NVIDIA RTX 4070.

5.3 Results

As seen in Table 3, ABMIL outperforms all models tested, including CNN.

As expected, the random forest with summary statistic feature engineering performs much worse than with clustering feature engineering. However, it is interesting that the random forest with clustering feature engineering presents such good performance. The clustering approach appears to catch clonal populations that would indicate myeloma.

The performance advantage of the ABMIL model over the CNN is likely because the ABMIL model can handle more events for a better representation of the flow cytometry data.

As seen in Table 4, our performance for the ABMIL model was worse than the performance reported for the external ABMIL model trained on leukemia flow cytometry files [3]. The authors did not report a precision or F1 score. However, we can see that our model had a much lower recall score, indicating it likely makes more false negative predictions than the external model.

6 Analysis

Based on Figure 1, the precision and recall have a large trade-off with each other.

We can see based on Figure 2 that the false positive rate for our ABMIL model begins to increase drastically with true positive rate.

The confusion matrix in Figure 3 confirms that we have more false negatives than false positives. This is a big concern for the application of the model since the consequences of false negative results mean that patients are not informed that they have myeloma when they do, and this leads to patients getting delayed or no treatment which can lead to the cancer spreading or becoming fatal.

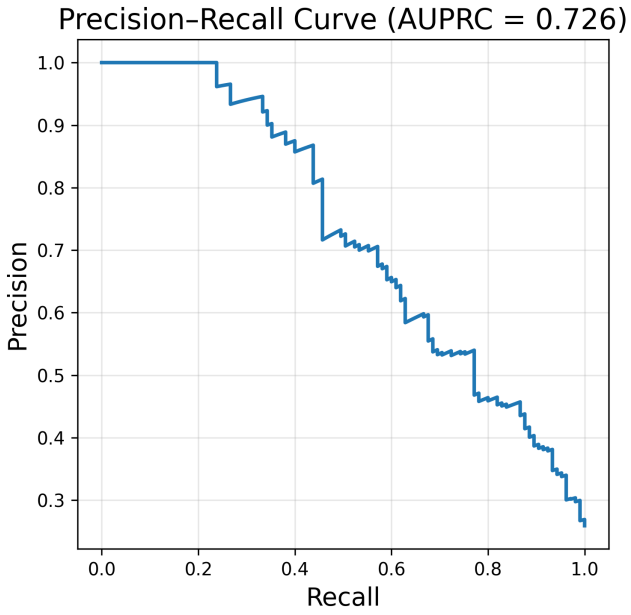

Figure 1: Precision-recall curve for ABMIL.

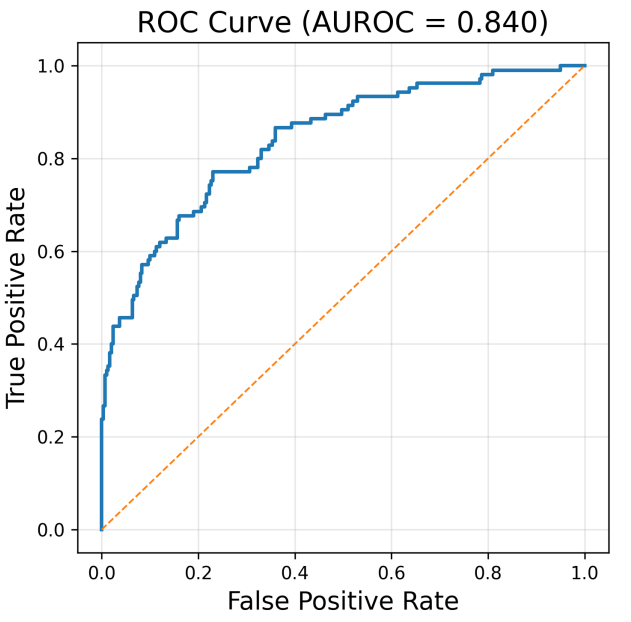

Figure 2: ROC curve for ABMIL.

Table 3: Performance of All Models

Model	Precision	Recall	F1 Score	AUROC	Accuracy
Random Forest (Summary)	0.69	0.23	0.34	0.60	0.58
Random Forest (Clustering)	0.76	0.42	0.54	0.82	0.81
Convolutional Neural Network	**0.93**	0.26	0.40	0.75	0.80
ABMILM	0.72	**0.46**	**0.56**	**0.84**	**0.84**

Table 4: Performance of Internal ABMIL Compared to External ABMIL

Model	Precision	Recall	F1 Score	AUROC	Accuracy
ABMILM	0.72	0.46	0.56	0.84	0.84
External ABMILM	-	**0.88**	-	**0.96**	**0.90**

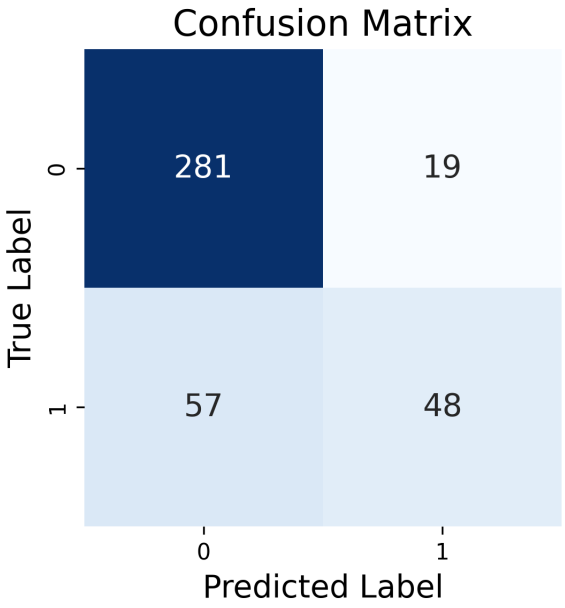

Figure 3: Confusion matrix for ABMIL.

6.1 Discussions

Our ABMIL model faces challenges in detecting special subpopulations of cells that would lead to better classification of positive myeloma cases. Mislabeled patients due to our preprocessing pipeline could be introducing errors that our model cannot avoid due to the upstream data issue.

Our current ABMIL model makes too many false negative predictions to be appropriate for a clinical setting. Once the model can produce a reasonable recall score, even at the cost of some more false positives, pathologists can apply ABMIL as a new tool for the diagnosis of myeloma.

Future work can take advantage of cleaner data with stronger and more confident labels. Clonal population subtyping (monoclonal, polyclonal, etc.) can also provide valuable information for pathologists to form their diagnosis regardless of disease predictive capabilities.

7 Conclusion

We present an attention-based multiple instance learning model to automate flow cytometry interpretation for myeloma detection. The ABMIL model outperforms all models it was tested against, which included traditional machine learning (random forest) and other deep learning architectures (convolutional neural network). ABMIL allows medical professionals to get an interpretation for a flow cytometry panel without the time-consuming and complicated process of manual preparation and interpretation of flow cytometry data.

Despite outperforming all other models, the model still struggles to detect positive cases of myeloma. We plan to make the model more sensitive to positive cases by adding better labeling of data and creating a novel architecture based on ABMIL.

Acknowledgments

A special thank you to Dr. David Jaye and Dr. Brooj Abro for sourcing the data for this project and providing vital background information in pathology. Thank you to Dr. Jinho D. Choi for an important introduction to professional AI research and to Dr. Carl Yang for encouraging the development of this project.

References

[1] Fu-Ming Cheng, Shih-Chang Lo, Ching-Chan Lin, Wen-Jyi Lo, Shang-Yu Chien, Ting-Hsuan Sun, and Kai-Cheng Hsu. 2024. Deep learning assists in acute leukemia detection and cell classification via flow cytometry using the acute leukemia orientation tube. *Scientific Reports* (2024).

[2] Maximilian Ilse, Jakub M. Tomczak, and Max Welling. 2018. Attention-based Deep Multiple Instance Learning. *CoRR* abs/1802.04712 (2018). arXiv:1802.04712 http://arxiv.org/abs/1802.04712

[3] Joshua E. Lewis, Lee A.D. Cooper, David L. Jaye, and Olga Pozdnyakova. 2024. Automated Deep Learning-Based Diagnosis and Molecular Characterization of Acute Myeloid Leukemia Using Flow Cytometry. *Modern Pathology* 37, 1 (Jan. 2024). doi:10.1016/j.modpat.2023.100373

[4] Sara A Monaghan, Jeng-Lin Li, Yen-Chun Liu, Ming-Ya Ko, Michael Boyiadzis, Ting-Yu Chang, Yu-Fen Wang, Chi-Chun Lee, Steven H Swerdlow, and Bor-Sheng Ko. 2021. A Machine Learning Approach to the Classification of Acute Leukemias and Distinction From Nonneoplastic Cytopenias Using Flow Cytometry Data. *American Journal of Clinical Pathology* 157, 4 (10 2021), 546–553. arXiv:https://academic.oup.com/ajcp/article-pdf/157/4/546/49103205/aqab148.pdf doi:10.1093/ajcp/aqab148

[5] David P. Ng, David Wu, Brent L. Wood, and Jonathan R. Fromm. 2015. Computer-Aided Detection of Rare Tumor Populations in Flow Cytometry: An Example With Classic Hodgkin Lymphoma. *American Journal of Clinical Pathology* 144, 3 (01 2015), 517–524. arXiv:https://academic.oup.com/ajcp/article-pdf/144/3/517/25001284/ajcpath144-0517.pdf doi:10.1309/AJCPY8E2LYHCGUFP

[6] David P Ng and Lauren M Zuromski. 2020. Augmented Human Intelligence and Automated Diagnosis in Flow Cytometry for Hematologic Malignancies. *American Journal of Clinical Pathology* 155, 4 (11 2020), 597–605. arXiv:https://academic.oup.com/ajcp/article-pdf/155/4/597/36603531/aqaa166.pdf doi:10.1093/ajcp/aqaa166

[7] Nicholas C. Spies, Alexandra Rangel, Paul English, Muir Morrison, Brendan O'Fallon, and David P Ng. 2025. Machine Learning Methods in Clinical Flow Cytometry. *Cancers* 17, 3 (Feb. 2025). doi:10.3390/cancers17030483